JOURNAL OF PURE AND APPLIED MICROBIOLOGY, Aug. 2015. Vol. **9**, p. 01-06
SPECIAL ISSUE ON RECENT RESEARCH CHALLENGES IN BIO-MEDICAL APPLICATIONS

Finite Element Modelling and Analysis of MRI Scan Knee Image using Soft Computing Techniques

V.K. Buvanesvari[1] and M. Suganthi[2]

[1]Anna University, Chennai, Tamilnadu, India.
[2]Department of Electronics and Communication Engineering,
Mahendra College of Engineering, Salem, Tamilnadu India.

(Received: 14 February 2015; accepted: 05 May 2015)

The knee is one of the largest and most complex joints in the body. The knee joins the thigh bone (femur) to the shin bone (tibia). The smaller bone that runs alongside the tibia (fibula) and the kneecap (patella) are the other bones that make the knee joint. Manual Material Handling (MMH), especially lifting, poses a risk to many and considered the prime cause of back pain and various other joint impairments. This in turn leads to increased worker compensation and loss of productive man-hours. Approximately one third of all jobs in industry involve MMH. Knee pain is one of the most prevalent and costly work related injure. The study of the Knee image during lifting of loads, the amounts of weight the man can safely lift are the areas concentrated on by Ergonomists. A biomechanical model of knee image has been developed, that can optimise the lifting posture for minimum effort. The model has been validated with practical data available from literature. This model can also be used to predict the lifting capabilities of individuals. This will be of great help to industrial managers for designing manual lifting tasks. A finite element model to study and analyse the stresses on Knee joint has also been developed. The effort to be taken for in vivo and in vitro data collection and analysis are reduced considerably in the finite element modelling.

Key words: Finite Element Analysis, Knee bone image, Ansys.

The knee joint is the largest bone in the body; it consists of four major bones and other network of muscles and ligaments. Injuries in the knee joint are mostly happened during sporting activities and understanding the anatomy of the joint is fundamental in understanding any subsequent pathology. The knee is made up of four main bones- the femur (thigh bone), the tibia (shin bone), fibula (outer shin bone) and patella (kneecap). The main movements of the knee joint occur between the patella, tibia and femur. All these parts are covered in articular cartilage which is known as extremely smooth and hard substance. It has been designed to gradually reduce the frictional forces as movement occurs between all the above bones. The patella is lies in an indentation at the lower end of the femur. It is known as the intercondylar groove. At the outer surface of the tibia lies the fibula, a long thin bone that travels right down to the ankle joint. Each knee joint has two crescent-shaped cartilage menisci. These lie on the medial (inner) and lateral (outer) edges of the upper surface of the tibia bone. These all the bones are essential and major components, acting as shock absorbers for the knee as well as allowing for correct weight distribution between the tibia and the femur. Edge detection is a fundamental tool used in most image processing applications to obtain information from the frames as a precursor step to feature extraction and object pre processing of segmentation. The segmentation process will detect outlines of the knee image and also indicates the boundaries by the way of

* To whom all correspondence should be addressed.
E-mail: v.k.buvanesvari@gmail.com
msuganthib@gmail.com

boundary line between the knee image and also the background of the image. An edge-detection median filter have been used to improve the appearance of blurred or anti-aliased images. The basic edge detection tool is used in this work known as matrix area gradient operator. It determines the level of variance between different pixels. Figure 1 shows the general description of knee image.

The edge-detection operator is calculated by forming a matrix cantered on a pixel chosen as the centre of the matrix area of the image. The calculated value of this image matrix area is indicated above a given threshold value, then the middle pixel is classified as a knee image edge. All these gradient-based algorithms have its own kernel operators that will calculate the strength of the slope which are orthogonal to each other, commonly vertical and horizontal. Later, the contributions of the different components of the slopes are combined to give the total value of the edge strength. Depending on the noise characteristics of the image or streaming video, edge detection results may also vary. Gradient-based type algorithms such as Sobel and Prewitt filter have a major drawback of being very sensitive to noise. Recent advances in computing technologies both in terms of hardware and software have helped in the advancement of CAD in applications beyond that of traditional design and analysis. CAD is now being used extensively in biomedical engineering in applications ranging from clinical medicine, customized medical implant design to tissue engineering[4]. The primary imaging modalities that are made use of in different applications include, computed tomography (CT), magnetic resonance imaging (MRI), optical microscopy, micro CT Scan, etc. Each of these methods having its own merits and demerits as described in the literature[1]. Using data derived from these images, computer models of human joints for stress analysis, dynamic force analysis and simulation; design of implants and scaffolds etc. have been reported in published literature[5]. This effort to model human body parts in a CAD based virtual environment is also referred to Image processing technique.

Proposed Work Sequence

The Block diagram of the proposed system of Image segmentation technique is shown in Figure 2. The different process sequence is involved in this segmentation is given in below. The Original image is obtained from the MRI scan image centre and then it will be incorporated by using CAD modelling and Image Parameters detection using canny edge detection algorithm. Both the results have been compared and analysed and obtained the best optimal value.

The filtering process carried out in this work is shown in the flow chart indicated in below figure 3.

Canny Edge Detection Algorithm

The Canny algorithm can be used an optimal edge detector based on a set of criteria which include finding the most edges by minimizing the error rate of the image, marking edges of the image is as closely as possible to the actual edges to maximize the localization of the image and marking image edges only one time when a single edge is exists for the purpose of minimal response. Based on the Canny Edge Detection algorithm, the optimal median filter that meets all three criteria above can be efficiently approximated using the first derivative of a Gaussian function.

$$GF(i,j) = \frac{1}{2\pi\sigma^2} e^{\frac{i^2+j^2}{2\pi\sigma^2}} \quad ...(1)$$

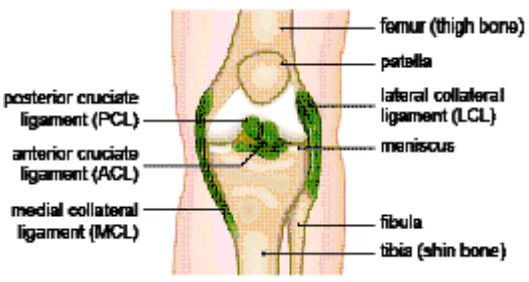

Fig.1. Knee Image General Description

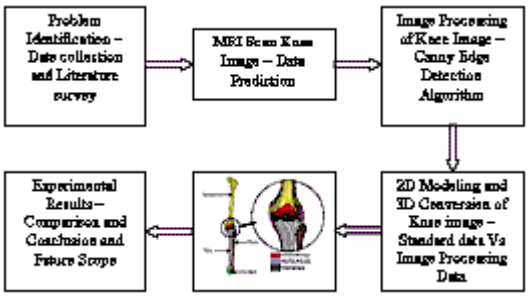

Fig. 2. Flow diagram of proposed method

$$\frac{\partial \mathbf{GF(i,j)}}{\partial \mathbf{i}} \ \alpha \mathbf{i} e^{\frac{i^2+j^2}{2\sigma^2}} \quad \frac{\partial \mathbf{GF(i,j)}}{\partial \mathbf{j}} \ \alpha j e^{\frac{i^2+j^2}{2\sigma^2}} \qquad ...(2)$$

All the images are having some speckle and other noises. So there is a need of noise filtering using any techniques. In this work median filter is used to reduce the noise. If the scan box is approximately centered with knee, the median filter is shown below.

$$C_i^j = Median\ (Pixel = P) \qquad ...(3)$$

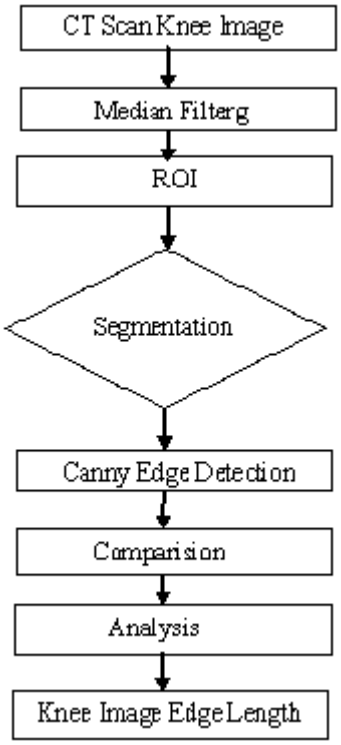

Fig. 3. Flow of filtering the Image

Where, the speckle noise reduction can be done using the below expression

$$SN_1^n = Pixel\ B_1^{n-1} \qquad ...(4)$$

Pre-processing of Initial Position of Edge parameters detection

Step 1: Calculate the average magnitude

$$\mathbf{M(1,2)} = \frac{\mathbf{1}}{M} \sum_{(1,2)}^{\mathbf{n}} \sqrt{\mathbf{Mx(1,2)^2 + My(1,2)^2}} \qquad ...(5)$$

Step 2: Calculate the edge length Density. The density value of the image edge length is calculated from

$$\mathbf{L(1,2)} = \frac{C(\mathbf{1,2})}{\max \mathbf{C(1,2)}} \qquad ...(6)$$

Where C(i,j) is the number of connected pixels at each position of pixel.

Step 3: Calculate the image Initial position of map from the summation of density of edge Length and average magnitude.

$$\mathbf{P(1,2)} = \frac{\mathbf{1}}{\mathbf{2}\left(M(\mathbf{1,2}) + L(\mathbf{1,2})\right)} \qquad ...(7)$$

Step 4: Calculate the thresholding of the initial position map. If

$$P(1,2) > T_{max} \qquad ...(8)$$

Then P(1, 2) is the initial position of the edge following. And then we obtained the initial position by setting T_{max} to 95% of the maximum value.

From the above figure 4(a) to 4(e) and the analysis we can able to predict the proper and suitable initial position, then the proposed

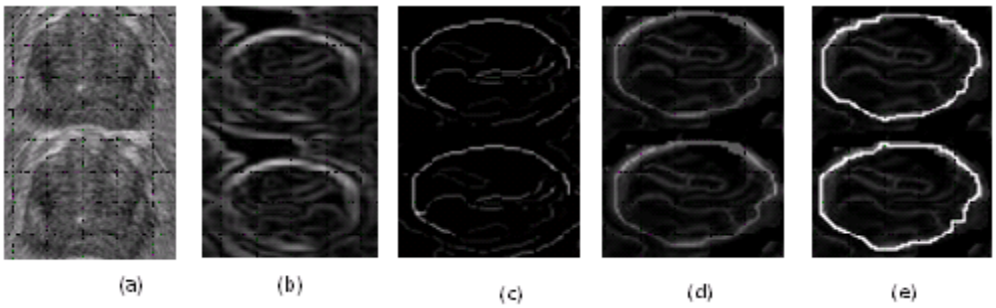

Fig. 4. (a). CT scan Noisy Knee image (b). Average Magnitude Image (c). Density of the Edge Length (d). Initial Position map (e). Final Thresholding of edge map

Table 1. Empirical Quantities of Knee bone

Material	Young's Modulus (Mpa)	Cross Section Area(mm^2)
Anterior Longitudinal	7.8	63.7
Posterior Longitudinal	10	20.0
Ligamentum Flavum	15	40.0
Transverse	10	3.60
Capsular	70.5	60.0
Interspinus	10	40.0
Superspinus	8	30.0
Iliolumbar	10	26.4

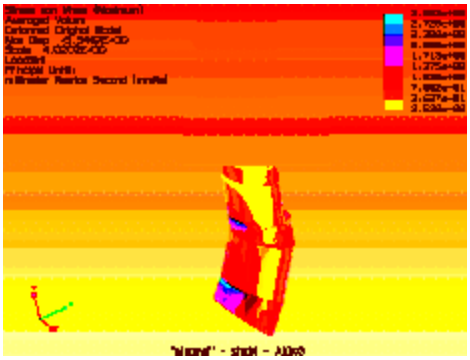

Fig. 4. Output image of knee joint using Ansys software during lifting of 10 kg loads

Table 2. Average Results of Probability of Error in Image Segmentation

S. No	Image Illustration	Canny Edge Detection (%)	Standard Value (%)	Error Difference DE (%)
1	Ultrasound Noisy Image	6.78	6.38	0.40
2	Right side Knee Image	9.83	8.99	0.84
3	Filtered Ultrasound Image	5.63	5.61	0.02
4	Edge Detection Noisy Image	5.41	5.37	0.05
5	Filtered Edge Detection Image	4.71	4.71	0.05
6	Fine Edge Filtered Image	4.62	4.62	0.05

technique will follow the edges until the closed and shaped contour is formed. With the above method, we can able to predict the dimension parameters of Knee image. With the help of these dimensions, we are going to prepare the two dimensional (2D) model of knee image for further stress analysis using AutoCAD software. Then the 2D image is to be converted to 3D image as per our sequence of work. Then 3D model is to be analysed using Pro/E software.

RESULTS AND DISCUSSION

Empirical quantities of knee bone are shown in table 1.

To further evaluate the efficiency of the proposed method in addition to the visual inspection, the proposed boundary detection method numerically using the Hausdorff distance and the probability of error in image segmentation. Where $P(O)$ and $P(B)$ are probabilities of objects and background in images. The objects surrounded by the contours obtained using the five snake models and the proposed method are compared with that manually drawn by skilled doctors from the Medical Hospital.

$$PE = P(O)P\left(\frac{B}{O}\right) + P(B)P\left(\frac{O}{B}\right) \quad ...(9)$$

From the above table 2 shows the average results of probability of Error in Image segmentation of canny edge detection algorithm and standard value also predicts the error difference for both the techniques.

CONCLUSION

The proposed technique for boundary detection and applied it to object segmentation problem in medical images. In this work we have used canny edge detection technique to incorporate a vector image model and the edge map information for the MRI scan knee image. The proposed technique was applied to detect the object boundaries in several types of noisy images where the well defined edges were found using this technique. Most of the synthetic and speckle noisy images were created and tested for the sake

of the known ground truths. The opinions of the skilled doctors were used as the ground truths of interesting objects in different types of medical images including prostates in ultra-sound images of knee images. The results of detecting the object boundaries in noisy images show that the proposed technique is much better. We have successfully applied the edge following technique to detect the object boundaries in medical images. And also we have predicted the stress value by using Ansys software. The proposed method can be applied not only for medical imaging problems; it may also be applied to other image processing problems.

REFERENCES

1. Camacho D.L.A., Hopper R.H., Lin G.M., Myers B.S., An Improved Method For Finite Element Mesh Generation Of Geometrically Complex Structures With Application To The Skull base, *Journal Of Biomechanics*, 1997; **30**(10): Pp. 1067–1070.
2. Carrigan S.D., Whiteside R.A., Pichora D.R., Small C.F., Development Of A Three-Dimensional Finite Element Model For Carpal Load Transmission In Static Neutral Posture, *Annals Of Biomedical Engineering*, 2003; **31**: Pp. 718–725.
3. Couteau B., Payan Y., Lavallee S., The Mesh-Matching Algorithm: An Automatic 3d Mesh Generator For Finite Element Structure, *Journal Of Biomechanics*, 2000; **33**(7): Pp. 1005–1009.
4. Keyak J.H., Meagher J.M., Skinner H.B., C.D.M. Jr., Automated Three-Dimensional Finite Element Modeling Of Bone: A New Method, *Journal Of Biomedical Engineering.*
5. Homminga J., Osteoporosis Changes The Amount Of Vertebral Trabecular Bone At Risk Of Fracture But Not The Vertebral Load Distribution, *Spine*, 2001; **26**(14): Pp. 1555–1561.
6. Silva M., Keaveny T.M., Hayes W.C., Load Sharing Between The Shell And Centrum In The Lumbar Vertebral Body, *Spine*, 1997; **22**(2): Pp. 140–150.
7. Lee K.K., Teo E.C., Effects Of Laminectomy And Facetectomy On The Stability Of The Lumbar Motion Segment, *Medical Engineering And Physics*, 2004; **26**(3): Pp. 183–192.
8. Zander T., Rohlmann A., Bergmann G., Influence Of Ligament Stiffness On The Mechanical Behavior Of A Functional Spinal Unit, *Journal Of Biomechanics*, 2004; **37**(7): Pp. 1107–1111.
9. Sept. 1990, 12, pp. 389–397.Helander M.G., Billingsley P.A. and Schurick J.M. (1984), 'An evaluation of human factors research in the workplace', *Human factors Review,* **1**: pp. 55-129.
10. Miller J.A. and Albert B. Schultz, 'Biomechanics of Human spine', Basic orthopaedic Biomechanics', 2nd Edition, Lippincott – Raven publishers, 1997; pp. 353-385.
11. Oliver J. and Middleditch A. 'Functional Anatomy of the spine', Butterworth Heinemann, 1991; pp. 1 – 79.
12. Williams J.R., Natarajan R.N., Anderson G.B.J. 'Biomechanical Response of a Lumbar Motion Segment Under Repetitive Loading conditions - A Finite Element study', Tenth Annual Symposium on Computational Methods in Orthopaedic Biomechanics, university of Texas south western Medical Center, Dallas 2002.
13. J. Guerrero, S.E. Salcudean, J.A. McEwen, B.A. Masri, and S. Nikolaou, Real-time vessel segmentation and tracking for ultrasound imaging applications, *IEEE Trans. Medical Imaging*, 2007; **26**(8): pp. 1079-1090.
14. N. Theera-Umpon and P. D. Gader, System level training of neural networks for counting white blood cells, *IEEE Trans. Syst., Man, and Cyber. Part C: App. and Reviews*, 2002; **32**(1): pp. 48-53.
15. J. Carballido-Gamio, S.J. Belongie, and S. Majumdar, Normalized cuts in 3-D for spinal MRI segmentation, *IEEE Trans. Medical Imaging*, 2004; **23**(1): pp. 36-44.
16. H. Greenspan, A. Ruf, and J. Goldberger, Constrained Gaussian mixture model framework for automatic segmentation of MR brain images, *IEEE Trans. Medical Imaging*, 2006; **25**(9): pp. 1233-1245.
17. J.-D. Lee, H.-R. Su, P.E. Cheng, M. Liou, J. Aston, A.C. Tsai, and C.-Y. Chen, MR image segmentation using a power transformation approach, *IEEE Trans. Medical Imaging*, 2009; **28**(6): pp. 894-905.
18. P. Jiantao, J.K. Leader, B. Zheng, F. Knollmann, C. Fuhrman, F.C. Sciurba, A computational geometry approach to automated pulmonary fissure segmentation in CT examinations, *IEEE Trans. Medical Imaging*, 2009; **28**(5): pp. 710-719.
19. Armentani E, Caputo E and Citarella R, 'Fem Sensitivity Analysis on the Stress Levels in a Human mandible with a varying ATM Modeling Complexity', *The open Mechanical Engineering Journal*, 2010; **4**: pp.8-15.
20. Sun W, Starly B, Nam J and Darling A, 'Bio-CAD modeling and its applications in computer-

aided tissue engineering', *Elsevier Journal of Computer Aided Design*, 2005; **37**: pp. 1097-1114.

21. Ciprian Radu and Ileana Rosca, 'Some contributions to the design of Osteo synthesis implants', *Estonian Journal of Engineering*, 2009; **15**: pp. 121-130.

22. Andras Hajdu, Janos Kormos and Zsolt Lencse, 'The MEDIP- Platform Independent Software System for Medical Image Processing Project', *Journal of Universal Computer Science,'* 2006; **12**(9): pp.1229-1239.